

# 3D Open-Vocabulary Panoptic Segmentation with 2D-3D Vision-Language Distillation

Zihao Xiao<sup>1\*</sup> Longlong Jing<sup>2</sup> Shangxuan Wu<sup>2</sup> Alex Zihao Zhu<sup>2</sup>  
Jingwei Ji<sup>2</sup> Chiyu Max Jiang<sup>2</sup> Wei-Chih Hung<sup>2</sup> Thomas Funkhouser<sup>3</sup>  
Weicheng Kuo<sup>4</sup> Anelia Angelova<sup>4</sup> Yin Zhou<sup>2</sup> Shiwei Sheng<sup>2</sup>

<sup>1</sup> Johns Hopkins University    <sup>2</sup> Waymo LLC    <sup>3</sup> Google Research    <sup>4</sup> Google DeepMind

## Abstract

3D panoptic segmentation is a challenging perception task, which aims to predict both semantic and instance annotations for 3D points in a scene. Although prior 3D panoptic segmentation approaches have achieved great performance on closed-set benchmarks, generalizing to novel categories remains an open problem. For unseen object categories, 2D open-vocabulary segmentation has achieved promising results that solely rely on frozen CLIP backbones and ensembling multiple classification outputs. However, we find that simply extending these 2D models to 3D does not achieve good performance due to poor per-mask classification quality on novel categories. In this paper, we propose the first method to tackle 3D open-vocabulary panoptic segmentation. Our model takes advantage of the fusion between learnable LiDAR features and dense frozen vision CLIP features, using a single classification head to make predictions for both base and novel classes. To further improve the classification performance on novel classes and leverage the CLIP model, we propose two novel loss functions: object-level distillation loss and voxel-level distillation loss. Our experiments on the nuScenes and SemanticKITTI datasets show that our method outperforms strong baselines by a large margin.

## 1. Introduction

3D panoptic segmentation is a crucial task in computer vision with many real-world applications, most notably in autonomous driving. It combines 3D semantic and instance segmentation to produce per-point predictions for two different types of objects: *things* (e.g., car) and *stuff* (e.g., road). To date, there has been significant progress in 3D panoptic segmentation [26, 39, 40, 44, 49, 54]. Most recently, methods such as [44] produce panoptic segmentation predictions directly from point clouds by leveraging

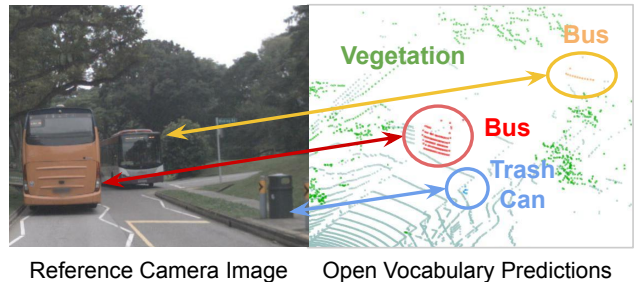


Figure 1. An illustration of open-vocabulary 3D panoptic segmentation results from our model. Without training on the categories of bus, trash can or vegetation, our method can produce accurate panoptic segmentation results even when the points are sparse.

learned queries to represent objects and Transformer [42]-based architectures [2, 4] to perform the modeling. However, existing models only predict panoptic segmentation results for a closed-set of objects. They fail to create predictions for the majority of unseen object categories in the scene, hindering the application of these algorithms to real-world scenarios. Recent advancements in vision-language (V-L) models [21, 38] have brought researchers’ attention to open-world computer vision tasks [3]. In 2D vision, there have been many successful methods in open-vocabulary object detection [11, 14, 23] and segmentation [10, 47, 51]. These methods learn to make predictions in a shared image-text embedding space, where predictions for unseen categories are produced by comparing the cosine similarity of an object with the text embedding of the category name. However, these methods are only possible due to the vast amounts of paired image-text data available, making it difficult to train similar models for 3D data such as LiDAR.

Instead, researchers have continued to leverage the effectiveness of these 2D vision-language models for 3D with the help of pixel-point correspondences by running inference on 2D images and then aligning with the 3D features. These methods have achieved promising results on open-vocabulary semantic segmentation [9, 34, 50, 52]

\*Work done while an intern at Waymo.

and instance segmentation [9, 50], individually. However, there are no methods that address the problem of 3D open-vocabulary panoptic segmentation, *i.e.*, addressing both open-vocabulary semantic segmentation and open-vocabulary instance segmentation at the same time. The challenge lies in how to handle segmentation for novel *things* and *stuff* simultaneously.

3D open-vocabulary panoptic segmentation is a challenging problem, both due to the significant domain gaps between the camera and LiDAR modalities and existing unsolved problems in open vocabulary segmentation. Many existing open-vocabulary works rely on similarities between text embeddings of class names and pre-trained V-L features to obtain associations between predictions and classes. However, while projecting 2D V-L features to 3D can account for a large part of the scene, there are often many points unaccounted for due to unmatched pixel / point distributions and differing fields of view between sensors. Many prior works rely entirely on the V-L features to perform both mask generation and object classification. While they work reasonably well, V-L models such as CLIP are trained at the image level, and so often suffer when tasked with fine-grained point or pixel level tasks.

In this work, we aim to address these two issues with a novel architecture for 3D Open-Vocabulary Panoptic Segmentation. Building on existing 3D closed-set panoptic segmentation methods, we train a learned LiDAR feature encoder in parallel with a frozen, pre-trained camera CLIP model. By fusing the 3D LiDAR features with the 2D CLIP features, our model is able to learn rich features throughout the entire 3D sensing volume, even if there are no camera features in certain regions. In addition, we apply a pair of novel distillation losses that allow the 3D encoder to learn both object-level and voxel-level features which live inside the CLIP feature space. This provides a learned module in 3D space which can directly be compared with text embeddings. In addition, these losses also provide useful training supervision to unknown parts of the scene where there would otherwise be no loss gradient.

With the proposed model and loss functions, our method significantly outperforms the strong baseline on multiple datasets. Our contributions are summarized as follows:

- We present the first framework for open-vocabulary 3D panoptic segmentation.
- We propose two novel loss functions, object-level distillation loss and voxel-level distillation loss to help novel object detection for both *things* and *stuff* classes.
- We experimentally show that our proposed method significantly outperforms that strong baseline model on both nuScenes and SemanticKITTI datasets.

## 2. Related Work

This work is closely related to 3D panoptic segmenta-

tion, 2D open-vocabulary segmentation, and 3D open-vocabulary segmentation and detection.

**3D panoptic segmentation.** The goal of 3D panoptic segmentation is to group 3D points according to their semantics and identities. This is a challenging task and relies on a good representation of the 3D data [1, 19, 35, 36, 41, 43, 45]. Most panoptic segmentation models have separate branches for instance segmentation and semantic segmentation [18, 26, 41, 54]. By following DETR [5], the recently proposed P3Former [44] uses learnable queries and a transformer architecture to obtain state-of-the-art performance on multiple panoptic segmentation benchmarks. Although those closed-set methods achieve incredible results, they cannot predict the labels and masks for novel classes.

**2D open-vocabulary segmentation.** 2D open vocabulary segmentation aims to group image pixels according to their semantics or identities for base (seen) or novel (unseen) categories. The prediction on novel categories is usually done by leveraging large V-L models [21, 38]. There are many works that focus on open vocabulary semantic segmentation [13, 16, 25, 28, 30, 33, 46, 48, 53, 55, 56]. Some work has also explored open-vocabulary panoptic segmentation [10, 37, 47]. Recently, FC-CLIP [51] proposes a single-stage framework based on a frozen convolutional CLIP backbone [20, 31, 38] for 2D open-vocabulary panoptic segmentation that achieves state-of-the-art performance. However, due to the camera-LiDAR domain gap, our experiments show that simply extending this 2D method to 3D leads to poor performance.

**3D open-vocabulary segmentation.** 3D open-vocabulary segmentation is less explored due to the lack of 3D point-to-text association. One common practice is to utilize V-L models and use 2D-3D pairings to obtain rich, structured information in 3D [6, 7, 9, 15, 17, 34, 50, 52]. Notably, CLIP2Scene[6] proposes a semantic-driven cross-modal contrastive learning framework. PLA [9] leverages images as a bridge and builds hierarchical 3D-caption pairs for contrastive learning. OpenScene [34] extracts per-pixel CLIP features using a pre-trained V-L model [13, 25] then derives dense 3D features by projecting 3D points onto image planes. One unpublished concurrent work, Region-PLC [50], utilize regional visual prompts to create dense captions and perform point-discriminative contrastive learning, which can be used for semantic segmentation or instance segmentation, individually. In contrast, our work does not rely on any captioning model or extra contrastive learning, only pre-trained CLIP features. Our model also simultaneously handles semantic and instance segmentation.

## 3. Method

This section is organized as follows. First, we define the 3D open-vocabulary panoptic segmentation task. We then provide detailed descriptions of the model architecture as

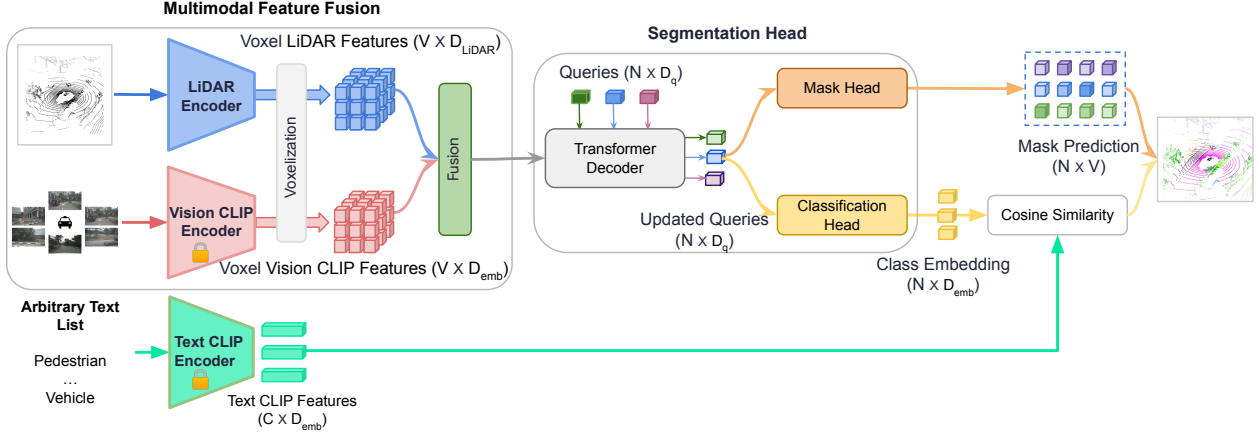


Figure 2. Overview of our method. Given a LiDAR point cloud and the corresponding camera images, LiDAR features are extracted with a learnable LiDAR encoder, while vision features are extracted by a frozen CLIP vision model. The extracted LiDAR features and the frozen CLIP vision features are then fused and fed to a query-based transformer model to predict instance masks and semantic classes.

well as the proposed loss functions. The overview of our method is presented in Fig. 2, and the two proposed loss functions are illustrated in Fig. 3 (a) and Fig. 3 (b).

### 3.1. Problem Definition

In 3D panoptic segmentation, the goal is to annotate every point in a point cloud. For *stuff* classes, (e.g. road, vegetation), a category label is assigned according to its semantics. For *things* classes (e.g. cars, pedestrians), an instance label is assigned to objects in addition to its semantic label.

In open-vocabulary panoptic segmentation, the models are trained on  $C_B$  base categories. At test time, besides these  $C_B$  base categories, the data will contain  $C_N$  novel categories. Following the settings of prior work [14, 23, 51], we assume the availability of the name of the novel categories during inference, but the novel categories are not present in the training data and their names are not known. Note that we do not apply any prompt engineering, as this is not the focus of this paper. We follow OpenScene [34] and obtain the CLIP Text embedding for each category.

### 3.2. 3D Open-Vocabulary Panoptic Segmentation

As there is no existing work for the 3D open vocabulary panoptic segmentation task, a natural idea would be extending the 2D open vocabulary segmentation methods to build the 3D counterpart. We start with P3Former [44], a state-of-the-art transformer-based 3D closed-set panoptic segmentation model, and add the essential components to support open-vocabulary capability by following FC-CLIP [51], a 2D open-vocabulary segmentation model that achieves state-of-the-art performance on multiple datasets. However, we found that this simple extension leads to poor performance in our experiments, and in this work we propose several new features to improve the performance of our model. More implementation details for this baseline

can be found in the supplementary material.

In order to improve the open vocabulary capability of our model, we propose significant changes to the P3Former architecture, as well as two new loss functions. The architecture of our method is shown in Fig. 2 and mainly consists of multimodal feature fusion, a segmentation head, and input text embeddings for open-vocabulary classification.

**Multimodal feature fusion.** The core idea of many recent 2D open-vocabulary works is to leverage the features of large-scale vision-language models [21, 38]. These methods [51] mainly rely on frozen CLIP features and use a transformer model to perform the 2D panoptic segmentation task. However, this is not optimal for 3D tasks since many points do not have corresponding valid camera pixels, leading to invalid features preventing meaningful predictions. To fully exploit the power of the CLIP vision features and learn complementary features from both CLIP features from camera and features from LiDAR, we generate predictions from the fusion of CLIP features extracted by a frozen CLIP model and learned LiDAR features from a LiDAR encoder.

As shown in Fig. 2, there are three major components for the multimodal feature fusion including a LiDAR encoder, a vision CLIP encoder, and voxel-level feature fusion. The LiDAR encoder is a model which takes an unordered set of points as input and extracts per-point features. We apply voxelization to the features from the LiDAR encoder, producing output features  $F_{lidar} \in \mathbb{R}^{V \times D_{lidar}}$ , where  $V$  is the number of the voxels and  $D_{lidar}$  is the dimension of the learned LiDAR feature. The Vision CLIP encoder is a pre-trained V-L segmentation model [13] which extracts pixel-wise CLIP features from each camera image. Within each voxel, every LiDAR point is projected into the camera image plane based on the intrinsic and extrinsic calibration parameters to index into the corresponding vision CLIP features, then the vision CLIP features of all the points be-

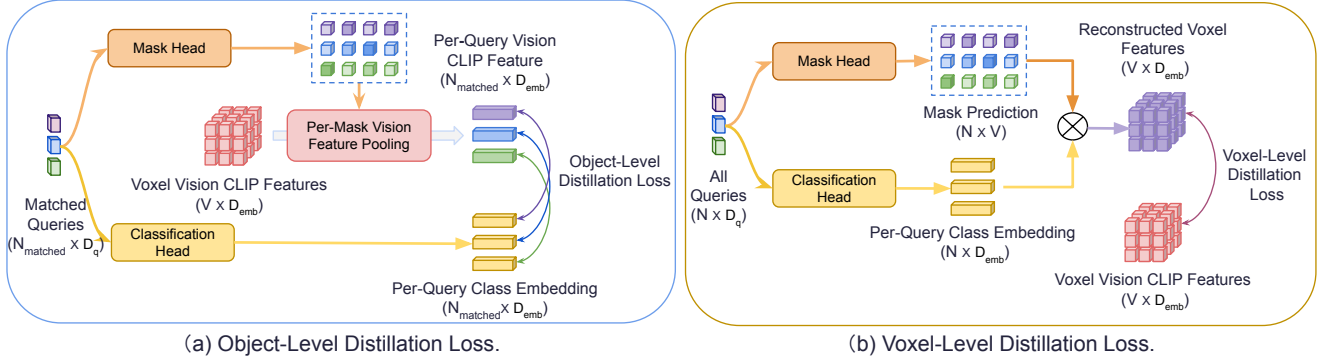


Figure 3. (a) the proposed object-level distillation loss, and (b) the proposed voxel-level distillation loss.

longing to each voxel are averaged to represent that voxel. Zero padding is used for points which do not have any valid corresponding camera pixels. The voxel CLIP features will be referred as  $F_{vclip} \in \mathbb{R}^{V \times D_{emb}}$ , where  $V$  is the number of voxels after voxelization and  $D_{emb}$  is the dimension of the CLIP features. Finally, the learned per-voxel LiDAR features and frozen per-voxel vision CLIP features are concatenated together to be used as input into the transformer decoder in the segmentation head. This feature fusion enables our model to learn complementary information from both the LiDAR and CLIP features, allowing us to fine-tune our backbone for each dataset’s specific data distribution.

**Segmentation head.** The segmentation head is a transformer model that takes the LiDAR-Vision fused feature as input to produce panoptic segmentation results. Prior works, including existing 2D open-vocabulary works such as FC-CLIP [51], typically use learnable queries  $q$  to represent each instance or thing, and they contain a mask prediction head  $f_{mask}$  to produce the corresponding mask for each individual object and a classification head  $f_{cls}$  to predict the per-mask class score for each known class. However, as a result, they also need to rely on another classifier to handle novel categories. Our goal is to use a single model to handle the prediction for both base and novel categories. Thus, we predict a class embedding instead of a class score for each mask. During training, the model learns to regress an analogy to the CLIP vision embedding for each mask, and the category prediction can be obtained by calculating its similarity with the CLIP text embedding of text queries during the inference stage. The class embedding  $f_{cls}$  prediction is defined as:

$$v_q = f_{cls}(q) \in \mathbb{R}^{D_{emb}}, \quad (1)$$

where  $v_q$  is in the CLIP embedding space. The predicted class logits are then computed from the cosine similarity between the predicted class embedding and the text embedding of every category name from the evaluation set using a frozen CLIP model. The classification logits are defined as:

$$s_{v_q} = \frac{1}{T} [\cos(v_q, t_1), \cos(v_q, t_2), \dots, \cos(v_q, t_C)] \quad (2)$$

where  $t_i \in \mathbb{R}^{D_{emb}}$ ,  $i \in \{1, 2, \dots, C\}$  is the text embedding,  $C$  is the number of categories ( $C_B$  in training and  $C_B + C_N$  in testing), and  $T$  is a learnable temperature term that controls the concentration of the distribution.

**Query assignment.** A common practice [8, 51] for transformer-based panoptic segmentation models is to utilize a single set of queries to make predictions for both *things* and *stuff* classes jointly. In contrast, P3Former uses one query set to represent *things* classes after bipartite matching and one fixed query set for *stuff* classes. We have found that this separation of *things* queries and *stuff* queries makes our model converge faster and improve overall performance, and similar pattern has been observed in other tasks [27]. However, the fixed set of queries for *stuff* classes is not applicable to the open-vocabulary setting due to the unknown number of novel *stuff* classes. To take advantage of the benefits of separating *things* queries and *stuff* queries, we propose to predict the base *stuff* classes with a fixed set of queries and utilize a set of learnable queries to target base *things* classes and all novel (*things* and *stuff*) classes. More details of the query assignment can be found in the supplementary materials.

### 3.3. Loss Function

Closed-set panoptic segmentation models [44] are typically optimized with objective functions consisting of a classification loss  $L_{cls}$  and a mask prediction loss  $L_{mask}$ . We follow P3Former [44] for these two losses: the classification loss  $L_{cls}$  optimizes the focal loss [29] between the class predictions and the category labels, while the mask loss  $L_{mask}$  optimizes the voxel-query classification loss. Besides the two standard loss functions, we propose two new losses to apply distillation from the CLIP model at different levels.

#### 3.3.1 Object-Level Distillation Loss

Similar to previous methods, our method uses the cosine similarity between predicted class embeddings and class text CLIP embeddings to produce per-class similarity

scores. However, the classification loss applied to Eq. (2) only enforces similarity to known classes. In this work, we make the assumption that the frozen CLIP features are discriminative with respect to open-vocabulary classes and have good out-of-distribution generalization. With this in mind, we propose an additional training loss which forces our predicted object-level class embeddings to be similar to the CLIP embeddings within their corresponding masks after matching. Similar to [51], we utilize voxel vision CLIP features to get a meaningful embedding for each query  $q$  by mask pooling the Vision CLIP features:

$$w_q = \frac{1}{|M_q|} \sum_p \mathbb{1}(p \in M_q) F_{vclip}(p) \quad (3)$$

where  $M_q$  is the set of points  $p$  belonging to the mask for query  $q$ . Our object-level distillation loss is then defined as:

$$L_O = \frac{1}{|Q_{matched}|} \sum_{q \in Q_{matched}} 1 - \cos(v_q, w_q), \quad (4)$$

where  $Q_{matched}$  is the set of queries matched with ground truth objects during training,  $v$  is the set of predicted class embeddings, and  $w$  is the set of mask-pooled CLIP embeddings. This loss forces the model to directly distill object-level camera CLIP features and improves model performance for novel *things* classes. We also experimented with applying  $L_O$  to all predicted masks, but we found that this reduced model performance, likely due to the presence of masks that do not correspond to any objects in the scene.

### 3.3.2 Voxel-Level Distillation Loss

While the object-level distillation loss distills the per-object features from CLIP model, it does not provide any supervision for the mask prediction head, which would otherwise only receive supervision for known classes. We found this particularly problematic for unknown *stuff* classes, which tend to be more spread out and cover larger and more diverse parts of the scene. In addition, it is only being applied to queries with relatively accurate mask predictions in order to learn useful CLIP features. To target these issues, we propose the voxel-level distillation loss to explicitly learn voxel-level CLIP features, which does not depend on any labels and can be applied on all queries. In particular, the voxel-level distillation loss is defined as:

$$F_{rec} = M_Q^T F_{Qemb} \quad (5)$$

where  $Q$  is the number of queries,  $F_{Qemb} \in \mathbb{R}^{Q \times D_{emb}}$  is the predicted embedding for all queries and  $M_Q \in \mathbb{R}^{Q \times V}$  is the predicted per-voxel mask probabilities for all queries. The reconstructed features can be regarded as the weighted sum of all queries for each voxel. We then again supervise

these features with the voxel CLIP features:

$$L_V = L_1(F_{rec}, F_{vclip}) \quad (6)$$

Unlike the object-level distillation loss, which is only applied to queries with matched ground truth, this loss is applied to all predicted mask scores and queries. In our experiments, we found that this loss significantly improves performance on *stuff* categories in particular, likely as it does not require exact matches with the ground truth, which can be difficult for large *stuff* classes. However, this loss is still susceptible to noisy or low quality mask scores, and we found that larger weights for this loss can disrupt training.

Our final objective function can be written as:

$$L = w_\alpha * L_{cls} + w_\beta * L_{mask} + w_\lambda * L_O + w_\gamma * L_V \quad (7)$$

, where  $w_\alpha, w_\beta, w_\lambda, w_\gamma$ , are weights for the corresponding objective function.

## 3.4. Implementation Details

For the LiDAR Encoder and Segmentation Head, we follow the implementation of the state-of-the-art closed-set 3D panoptic segmentation method P3Former. For the Vision CLIP Encoder, we use OpenSeg[13], due to its remarkable performance on the recent open-vocabulary 3D semantic segmentation task [34]. For the Text CLIP Encoder, we use CLIP[38] with ViT-L/14[42] backbone, following other state-of-the-art open vocabulary works [34].

## 4. Experiments

Following the state-of-the-art closed-set 3D panoptic segmentation work, we conduct experiments and ablation studies on the nuScenes [4] and SemanticKITTI [2, 12] datasets.

### 4.1. Experimental Setting

**nuScenes.** The nuScenes dataset [4] is a public benchmark for autonomous driving tasks. It consists of 1000 run segments and is further divided into prescribed train/val/test splits. We use all key frames with panoptic labels in the training set (28130 frames) to train the model. Following the most recent state-of-the-art model P3Former [44], we evaluate the models on the validation set (6019 frames). There are a total of 16 labeled semantic classes, including 10 *things* class and 6 *stuff* classes.

**SemanticKITTI.** SemanticKITTI [2, 12] is the first large dataset for LiDAR panoptic segmentation for autonomous driving. We conduct experiments on the training and validation sets, where panoptic segmentation labels are available. 3D open-vocabulary methods often require point and pixel pairing. In the SemanticKITTI dataset, however, the ego-vehicle is only equipped with frontal cameras. Thus, we filter out the points that are not visible in the camera view

based on the provided camera parameters for both training and evaluation. There are 19 semantic classes, including 8 *things* classes and 11 *stuff* classes.

**Data split.** Both the nuScenes and SemanticKITTI datasets do not provide official base and novel class splits. Following the state-of-the-art 3D open-vocabulary segmentation work [9, 50], we randomly split the classes into base and novel, while keeping the ratio between base and novel classes around 3 : 1. For nuScenes, the number of class for base and novel split are 12 and 4 respectively, and this setting will be referred as B12/N4. For SemanticKITTI, the number of class for base and novel split are 14 and 5, and this setting will be referred as B14/N5. We use the same splits in the main comparison with prior methods, and provide the results of more variations in the ablation studies.

**Training details.** We follow most of the architecture configurations in the official P3Former[44] implementation. We set  $w_\alpha = 1$ ,  $w_\beta = 1$ ,  $w_\lambda = 1$ ,  $w_\gamma = 0.1$  for both datasets. We use the AdamW [22, 32] optimizer with a weight decay of 0.01. We set the initial learning rate as 0.0008 with a multi-step decay schedule. The models are trained for 40 epochs, and we use the checkpoint of the last epoch for evaluation. To avoid ambiguous class names and better utilize the CLIP text embedding, we follow [24, 34, 51] and apply multi-label mapping for the text queries. During inference, if there are multiple labels for one class, we derive the class score by getting the maximum scores among these labels.

**Evaluation metrics.** We use panoptic quality ( $PQ$ ) as the major evaluation metric for the panoptic segmentation task.  $PQ$  is formulated as:

$$PQ = \underbrace{\frac{\sum_{TP} \text{IoU}}{|TP|}}_{SQ} \times \underbrace{\frac{|TP|}{|TP| + \frac{1}{2}|FP| + \frac{1}{2}|FN|}}_{RQ}. \quad (8)$$

$PQ$  is the multiplication of segmentation quality ( $SQ$ ) and recognition quality ( $RQ$ ). We report all the three metrics ( $PQ$ ,  $RQ$ ,  $SQ$ ) for all classes. We also report  $PQ$ ,  $RQ$ ,  $SQ$  for novel *things* objects and novel *stuff* objects separately. In particular,  $PQ_N^{Th}$  means  $PQ$  for novel *things* classes and  $PQ_N^{St}$  stands for  $PQ$  for novel *stuff* classes. We also report the mean Intersection over Union (mIoU) for all classes to measure semantic segmentation quality.

## 4.2. P3Former+FC-CLIP Baseline

As a baseline for novel-class panoptic segmentation, we construct a baseline model from a fusion of P3Former [44] and FC-CLIP [51] – this baseline will be called P3Former+FC-CLIP (PFC). The baseline model takes the frozen voxel vision CLIP features as input, and the final prediction is obtained by geometric ensembling[13, 14, 23, 47, 51] of the results from the classification head  $f_{cls}$  and another classifier based on the similarity between the average-

pool class embedding  $w_q$  and the CLIP text embedding. Following FC-CLIP [51], the same set of learnable queries were used to represent both things and stuff classes. In summary, this baseline provides a comparison against our proposed method without the Multimodal Feature Fusion module, the unified Segmentation Head, and the distillation losses. More information on this baseline can be found in the supplementary material.

## 4.3. Main Results

Since there are no existing methods for the open vocabulary 3D panoptic segmentation task, we mainly compare with three methods to demonstrate the capability of our method: (1) the strong open-vocabulary baseline method PFC to fairly demonstrate the strength of our method, (2) the closed-set state-of-the-art 3D panoptic segmentation method P3Former to understand the headroom of our method, and (3) the open-set, zero-shot state-of-the-art method for 3D semantic segmentation, OpenScene [34]. Comparisons on the nuScenes and SemanticKITTI datasets are shown in Tab. 1 and Tab. 2.

### 4.3.1 Results on nuScenes Dataset

Tab. 1 shows the performance comparison on the validation set of the nuScenes dataset. Our method significantly outperforms the strong baseline PFC by a large margin across all metrics. PFC works relatively well for the novel *things* classes, but performance on the novel *stuff* class collapses. This is likely because *stuff* classes tend to cover large parts of the scene, leading to diverse per-voxel CLIP features which may not be good representatives for their respective classes. For the novel *stuff* classes, PFC only achieves 0.5  $PQ_N^{St}$ , while our method achieves 35.2. PFC can produce reasonable masks for the novel *stuff* classes (with  $SQ_N^{St}=60.4$ ), but fails to produce high quality semantic predictions for the novel *stuff* class (with  $RQ_N^{St}=0.8$ ). Fig. 4 shows a qualitative comparison between PFC and our method. With our proposed design, and especially the new loss functions, our method is able to achieve strong performance for both novel *things* and *stuff* classes.

To further understand the headroom of our method, we also compare with the closed-set P3Former. Note that the comparison here is deliberately unfair, and is intended for us to understand the headroom and limitations of our method.  $SQ$  indicates segmentation quality, and the gap between our method and P3Former is relatively small (less than  $10SQ$ ), but there is a large gap (over  $30RQ$ ) on the  $RQ$  metric, which represents mask classification quality. These gaps are largely due to regressions in the novel classes, with smaller margins for the base classes as shown in Tab. 3.

For the base classes, the gap is relatively small except for a drop in  $RQ_B^{Th}$ . We believe that the closed-set P3Former

Model	Type	Supervision	$PQ$	$PQ_N^{Th}$	$PQ_N^{St}$	$RQ$	$RQ_N^{Th}$	$RQ_N^{St}$	$SQ$	$SQ_N^{Th}$	$SQ_N^{St}$	mIoU
P3Former[44]	closed-set	full	75.9	85.1	82.9	84.7	89.9	95.9	89.8	94.7	86.5	76.8
OpenScene[34]	open-voc	zero-shot	-	-	-	-	-	-	-	-	-	42.1
PFC	open-voc	partial	54.8	37.3	0.5	63.6	42.1	0.8	84.2	<b>89.3</b>	60.4	55.5
Ours	open-voc	partial	<b>62.0</b>	<b>49.6</b>	<b>35.2</b>	<b>70.9</b>	<b>55.6</b>	<b>46.0</b>	<b>87.0</b>	89.1	<b>76.7</b>	<b>60.1</b>

Table 1. **Quantitative results of panoptic segmentation on nuScenes.** We compare the performance of open-vocabulary and fully supervised models. All open vocabulary models share the same randomly picked base/novel split: B12/N4. The novel *things* classes are bus, pedestrian and motorcycle. The novel *stuff* class is vegetation.

Model	Type	Supervision	$PQ$	$PQ_N^{Th}$	$PQ_N^{St}$	$RQ$	$RQ_N^{Th}$	$RQ_N^{St}$	$SQ$	$SQ_N^{Th}$	$SQ_N^{St}$	mIoU
P3Former[44]	closed-set	full	62.1	65.9	74.2	71.3	74.8	86.8	77.1	88.3	83.9	61.6
PFC	open-voc	partial	33.7	12.0	0.4	40.1	15.0	0.6	67.6	81.1	47.3	33.4
Ours	open-voc	partial	<b>42.2</b>	<b>13.1</b>	<b>17.8</b>	<b>50.4</b>	<b>16.2</b>	<b>26.7</b>	<b>73.0</b>	<b>84.0</b>	<b>67.2</b>	<b>44.6</b>

Table 2. **Quantitative results of panoptic segmentation on SemanticKITTI.** We compare the performance of open-vocabulary and fully supervised models. All open vocabulary models share the same randomly picked base/novel split: B14/N5. The novel *things* classes are bicycle and truck. The novel *stuff* classes are sidewalk, building and trunk.

Model	Data	Base Things			Base Stuff		
		$PQ_B^{Th}$	$RQ_B^{Th}$	$SQ_B^{Th}$	$PQ_B^{St}$	$RQ_B^{St}$	$SQ_B^{St}$
P3Former	All	73.4	80.5	90.9	73.9	85.3	85.9
P3Former	Base	65.2	71.3	88.0	64.2	77.4	81.8
PFC	Base	65.6	73.3	89.0	61.0	75.4	83.7
Ours	Base	66.7	73.7	89.8	69.2	82.1	83.7

Table 3. **Performance for base classes on nuScenes.** We report the performance on base classes for models in Tab. 1. A gap still exists between open and closed-set methods for base classes, particularly for  $RQ_B^{Th}$ . We show that this is due to lack of supervision of the whole scene as P3Former achieves similar performance when only trained on base categories.

sees ground truth supervision for the entire scene, while the open-set methods do not receive supervision in the ‘unknown class’ regions. When the P3Former is only trained on base categories, the performance is similar to the PFC baseline and it is slightly worse than our proposed method.

Besides the comparison with the closed-set method, we also compare with the zero-shot state-of-the-art method OpenScene [34] which does not use any labels for training. In this comparison, our model significantly outperforms OpenScene in the mIoU metric for semantic segmentation. Note that this comparison is not entirely fair, as our method is trained with partial labels. Instead, the comparison is useful to understand the gap between the two types of open-vocabulary methods. The unpublished RegionPLC [50] also reports open-vocabulary results for the semantic segmentation task on the nuScenes dataset; however, we cannot directly compare with this method since it removes one class (other-flat) and does not provide its base/novel split.

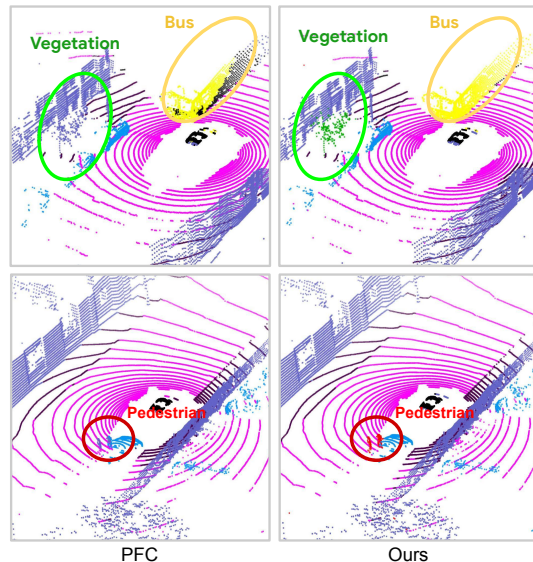


Figure 4. Open-vocabulary panoptic segmentation results from PFC and our method on nuScenes. The PFC predicts inaccurate category and masks for the novel pedestrian (red), bus (yellow) and vegetation (green), while ours makes correct predictions.

### 4.3.2 Results on SemanticKITTI Dataset

To demonstrate the generalization ability of our method across different datasets, we report the results on SemanticKITTI dataset in Tab. 2. Overall, we observe similar patterns as on the nuScenes dataset. The baseline achieves relatively poor overall performance and struggles with the novel *stuff* classes. Using our architecture and loss functions, our model significantly outperforms PFC on  $PQ$ , with the largest margin for novel *stuff* classes. Note that the gap between the open-vocabulary methods (ours and baseline) and the closed-set method is larger on SemanticKITTI,

Components				$PQ$	$PQ_N^{Th}$	$PQ_N^{St}$	$RQ$	$RQ_N^{Th}$	$RQ_N^{St}$	$SQ$	$SQ_N^{Th}$	$SQ_N^{St}$	mIoU
QA	Fusion	$L_O$	$L_V$										
				54.8	37.3	0.5	63.6	42.1	0.8	84.2	<b>89.3</b>	60.4	55.5
✓				55.5	35.7	0.4	64.0	40.8	0.7	84.3	87.4	56.5	56.6
✓	✓			56.4	38.1	0.4	65.0	43.5	0.6	84.6	87.4	61.3	56.4
✓	✓	✓		56.3	43.8	0.2	64.8	49.2	0.3	85.1	88.9	64.0	54.0
✓	✓	✓	✓	<b>62.0</b>	<b>49.6</b>	<b>35.2</b>	<b>70.9</b>	<b>55.6</b>	<b>46.0</b>	<b>87.0</b>	89.1	<b>76.7</b>	<b>60.1</b>

Table 4. **Impact of each component.** We evaluate the impact of each component using the base/novel split in Tab. 1. We observe that each component can provide improvements over the PCF baseline. Noticeably,  $L_V$  brings the biggest improvement.

Model	Type	Supervision	$PQ$	$PQ_N^{Th}$	$PQ_N^{St}$	$RQ$	$RQ_N^{Th}$	$RQ_N^{St}$	$SQ$	$SQ_N^{Th}$	$SQ_N^{St}$	mIoU
P3Former[44]	closed-set	full	75.8	70.5	71.7	83.8	76.4	85.5	90.1	91.6	83.6	75.0
PFC	open-voc	partial	43.9	27.7	0.6	51.7	33.2	1.0	80.2	82.4	62.7	45.2
Ours	open-voc	partial	<b>52.8</b>	<b>56.0</b>	<b>16.4</b>	<b>60.5</b>	<b>61.8</b>	<b>22.6</b>	<b>84.9</b>	<b>89.7</b>	<b>68.7</b>	<b>49.9</b>

Table 5. **Performance of panoptic segmentation on nuScenes with a different split.** We compare the performance with a different split with 5 novel classes (B11/N5). The novel *things* classes are bicycle, car and construction vehicle. The novel *stuff* classes are terrain and man-made. Our method consistently outperforms the PFC baseline across all the metrics by a large margin.

likely due to the smaller dataset limiting performance.

#### 4.4. Ablation Studies

To better demonstrate and understand the effectiveness of each component, we conduct ablation studies for each design choice and loss function on the nuScenes dataset. These results are shown in Tab. 4. In total, we conduct five sets of experiments, starting with the PFC baseline with separate base / novel classifiers and geometric ensemble, and build upon it four ablations with different combinations of design choice and loss functions.

**Impact of the query assignment.** Starting from the PFC baseline model, we add our proposed fixed query assignment for stuff categories. The results for this ablation are shown in the second row of Tab. 4. With query assignment, the overall  $PQ$  improves by 0.7, showing that it indeed helps the overall performance. The performance for the novel classes drop slightly, but improvement on the base classes overcomes this for the overall  $PQ$ .

**Impact of feature fusion.** The third row of Tab. 4 shows the impact of feature fusion. Without feature fusion, our model already achieves 55.5  $PQ$ , demonstrating the power of the CLIP vision features. The third row shows that the performance with feature fusion for the model input improves the overall  $PQ$  by 0.9. This slightly improved the overall performance, but the improvement on the novel *things* class is the most significant, demonstrating that the learned LiDAR features and CLIP vision features are indeed complementary for the task.

**Impact of the object-level distillation loss.** The fourth row of the results in Tab. 4 shows the impact of the proposed object-level distillation loss. In this ablation, we also remove the base class classification head and geometric ensemble, consolidating to a single class embedding head. Al-

though the  $RQ_N^{St}$  slightly dips by 0.3 for the novel *stuff* classes, this loss can significantly improve the  $RQ_N^{Th}$  for the novel *things* class by 5.7. Moreover, this loss helps improve the segmentation quality ( $SQ$ ) for both *things* and *stuff* classes.

**Impact of the voxel-level distillation loss.** We further study the impact of the voxel-level distillation loss to see if it can further improve the performance given all of our designs. The results are shown in the last row of Tab. 4. With this loss function, we can see that the  $PQ$  significantly improves by 5.7. The improvement on the novel split is particularly large, especially for the novel *stuff* classes. The  $PQ_N^{St}$  of the novel *stuff* class improves from 0.2 to 35.2 demonstrating the importance of the voxel-level supervision to the performance of the novel *stuff* class.

**Performance of different splits.** To validate the generalizability of our method across different base/novel class split, we conduct experiments on a different split (B11/N5) for the nuScenes dataset. Here, the five novel categories are bicycles, cars, construction vehicles, terrain, and man-made. As shown in Tab. 5, similar to the results on the other split (B12/N4), our proposed method consistently and significantly outperforms the strong baseline method by a large margin. This again demonstrates the effectiveness of our design and the proposed loss functions. However, we do notice that the performance of our method and the baseline drops when more classes are included into the novel split.

## 5. Conclusion

In this paper, we present the first system for the open vocabulary 3D panoptic segmentation task by leveraging large vision-language models. We experimentally verified that simply extending the 2D open-vocabulary segmen-



tation method into 3D does not yield good performance, and demonstrated that our proposed model design and loss functions significantly boost performance for this task. Our method significantly outperformed the strong baseline on multiple well-established benchmarks in the literature. We hope our work can shed light on the future studies of the 3D open-vocabulary panoptic segmentation problem.

**Acknowledgements.** We would like to thank Mahyar Najibi, Chao Jia, Zhenyao Zhu, Yolanda Wang, Charles R. Qi, Dragomir Anguelov, Tom Ouyang, Ruichi Yu, Chris Sweeney, Colin Graber, Yingwei Li, Sangjin Lee, Weilong Yang, and Congcong Li for the help to the project.

## References

- [1] Inigo Alonso, Luis Riazuelo, Luis Montesano, and Ana C Murillo. 3d-mininet: Learning a 2d representation from point clouds for fast and efficient 3d lidar semantic segmentation. *IEEE Robotics and Automation Letters*, 5(4):5432–5439, 2020. [2](#)
- [2] J. Behley, M. Garbade, A. Milioto, J. Quenzel, S. Behnke, C. Stachniss, and J. Gall. SemanticKITTI: A Dataset for Semantic Scene Understanding of LiDAR Sequences. In *ICCV*, 2019. [1](#), [5](#)
- [3] Abhijit Bendale and Terrance Boulton. Towards open world recognition. In *CVPR*, 2015. [1](#)
- [4] Holger Caesar, Varun Bankiti, Alex H Lang, Sourabh Vora, Venice Erin Liong, Qiang Xu, Anush Krishnan, Yu Pan, Giancarlo Baldan, and Oscar Beijbom. nuscenes: A multi-modal dataset for autonomous driving. In *CVPR*, 2020. [1](#), [5](#)
- [5] Nicolas Carion, Francisco Massa, Gabriel Synnaeve, Nicolas Usunier, Alexander Kirillov, and Sergey Zagoruyko. End-to-end object detection with transformers. In *ECCV*, 2020. [2](#)
- [6] Runnan Chen, Youquan Liu, Lingdong Kong, Xinge Zhu, Yuexin Ma, Yikang Li, Yuenan Hou, Yu Qiao, and Wenping Wang. Clip2scene: Towards label-efficient 3d scene understanding by clip. In *CVPR*, 2023. [2](#)
- [7] Zhimin Chen and Bing Li. Bridging the domain gap: Self-supervised 3d scene understanding with foundation models. *arXiv preprint arXiv:2305.08776*, 2023. [2](#)
- [8] Bowen Cheng, Alex Schwing, and Alexander Kirillov. Pixel classification is not all you need for semantic segmentation. In *NeurIPS*, 2021. [4](#)
- [9] Runyu Ding, Jihan Yang, Chuhui Xue, Wenqing Zhang, Song Bai, and Xiaojuan Qi. Pla: Language-driven open-vocabulary 3d scene understanding. In *CVPR*, 2023. [1](#), [2](#), [6](#)
- [10] Zheng Ding, Jieke Wang, and Zhuowen Tu. Open-vocabulary universal image segmentation with maskclip. In *ICML*, 2023. [1](#), [2](#)
- [11] Yu Du, Fangyun Wei, Zihe Zhang, Miaojing Shi, Yue Gao, and Guoqi Li. Learning to prompt for open-vocabulary object detection with vision-language model. In *CVPR*, 2022. [1](#)
- [12] A. Geiger, P. Lenz, and R. Urtasun. Are we ready for Autonomous Driving? The KITTI Vision Benchmark Suite. In *CVPR*, 2012. [5](#)
- [13] Golnaz Ghiasi, Xiuye Gu, Yin Cui, and Tsung-Yi Lin. Scaling open-vocabulary image segmentation with image-level labels. In *ECCV*, 2022. [2](#), [3](#), [5](#), [6](#), [11](#)
- [14] Xiuye Gu, Tsung-Yi Lin, Weicheng Kuo, and Yin Cui. Open-vocabulary object detection via vision and language knowledge distillation. *ICLR*, 2022. [1](#), [3](#), [6](#), [11](#)
- [15] Huy Ha and Shuran Song. Semantic abstraction: Open-world 3d scene understanding from 2d vision-language models. In *CoRL*, 2022. [2](#)
- [16] Wenbin He, Suphanut Jamonnak, Liang Gou, and Liu Ren. Clip-s4: Language-guided self-supervised semantic segmentation. In *CVPR*, 2023. [2](#)
- [17] Deepti Hegde, Jeya Maria Jose Valanarasu, and Vishal M Patel. Clip goes 3d: Leveraging prompt tuning for language grounded 3d recognition. *arXiv preprint arXiv:2303.11313*, 2023. [2](#)
- [18] Fangzhou Hong, Hui Zhou, Xinge Zhu, Hongsheng Li, and Ziwei Liu. Lidar-based panoptic segmentation via dynamic shifting network. In *CVPR*, 2021. [2](#)
- [19] Qingyong Hu, Bo Yang, Linhai Xie, Stefano Rosa, Yulan Guo, Zhihua Wang, Niki Trigoni, and Andrew Markham. Learning semantic segmentation of large-scale point clouds with random sampling. *IEEE Transactions on Pattern Analysis and Machine Intelligence*, 44(11):8338–8354, 2021. [2](#)
- [20] Gabriel Ilharco, Mitchell Wortsman, Ross Wightman, Cade Gordon, Nicholas Carlini, Rohan Taori, Achal Dave, Vaishaal Shankar, Hongseok Namkoong, John Miller, Hananeh Hajishirzi, Ali Farhadi, and Ludwig Schmidt. Openclip, 2021. [2](#)
- [21] Chao Jia, Yinfei Yang, Ye Xia, Yi-Ting Chen, Zarana Parekh, Hieu Pham, Quoc Le, Yun-Hsuan Sung, Zhen Li, and Tom Duerig. Scaling up visual and vision-language representation learning with noisy text supervision. In *ICML*, 2021. [1](#), [2](#), [3](#)
- [22] Diederik P Kingma and Jimmy Ba. Adam: A method for stochastic optimization. In *ICLR*, 2015. [6](#)
- [23] Weicheng Kuo, Yin Cui, Xiuye Gu, AJ Piergiovanni, and Anelia Angelova. F-vlm: Open-vocabulary object detection upon frozen vision and language models. In *ICLR*, 2023. [1](#), [3](#), [6](#), [11](#)
- [24] John Lambert, Zhuang Liu, Ozan Sener, James Hays, and Vladlen Koltun. Mseg: A composite dataset for multi-domain semantic segmentation. In *CVPR*, 2020. [6](#)
- [25] Boyi Li, Kilian Q Weinberger, Serge Belongie, Vladlen Koltun, and Rene Ranftl. Language-driven semantic segmentation. In *ICLR*, 2022. [2](#)
- [26] Jinke Li, Xiao He, Yang Wen, Yuan Gao, Xiaoqiang Cheng, and Dan Zhang. Panoptic-phnet: Towards real-time and high-precision lidar panoptic segmentation via clustering pseudo heatmap. In *CVPR*, 2022. [1](#), [2](#)
- [27] Zhiqi Li, Wenhai Wang, Enze Xie, Zhiding Yu, Anima Anandkumar, Jose M. Alvarez, Ping Luo, and Tong Lu. Panoptic segformer: Delving deeper into panoptic segmentation with transformers. In *CVPR*, 2022. [4](#)

- [28] Feng Liang, Bichen Wu, Xiaoliang Dai, Kungpeng Li, Yanan Zhao, Hang Zhang, Peizhao Zhang, Peter Vajda, and Diana Marculescu. Open-vocabulary semantic segmentation with mask-adapted clip. In *CVPR*, 2023. 2
- [29] Tsung-Yi Lin, Priya Goyal, Ross Girshick, Kaiming He, and Piotr Dollar. Focal loss for dense object detection. In *ICCV*, 2017. 4
- [30] Quande Liu, Youpeng Wen, Jianhua Han, Chunjing Xu, Hang Xu, and Xiaodan Liang. Open-world semantic segmentation via contrasting and clustering vision-language embedding. In *ECCV*, 2022. 2
- [31] Zhuang Liu, Hanzi Mao, Chao-Yuan Wu, Christoph Feichtenhofer, Trevor Darrell, and Saining Xie. A convnet for the 2020s. In *CVPR*, 2022. 2
- [32] Ilya Loshchilov and Frank Hutter. Decoupled weight decay regularization. In *ICLR*, 2019. 6
- [33] Chaofan Ma, Yuhuan Yang, Yanfeng Wang, Ya Zhang, and Weidi Xie. Open-vocabulary semantic segmentation with frozen vision-language models. *BMVC*, 2022. 2
- [34] Songyou Peng, Kyle Genova, Chiyu Jiang, Andrea Tagliasacchi, Marc Pollefeys, Thomas Funkhouser, et al. Openscene: 3d scene understanding with open vocabularies. In *CVPR*, 2023. 1, 2, 3, 5, 6, 7
- [35] Charles R Qi, Hao Su, Kaichun Mo, and Leonidas J Guibas. Pointnet: Deep learning on point sets for 3d classification and segmentation. In *CVPR*, 2017. 2
- [36] Charles Ruizhongtai Qi, Li Yi, Hao Su, and Leonidas J Guibas. Pointnet++: Deep hierarchical feature learning on point sets in a metric space. *NeurIPS*, 2017. 2
- [37] Jie Qin, Jie Wu, Pengxiang Yan, Ming Li, Ren Yuxi, Xuefeng Xiao, Yitong Wang, Rui Wang, Shilei Wen, Xin Pan, et al. Freeseg: Unified, universal and open-vocabulary image segmentation. In *CVPR*, 2023. 2
- [38] Alec Radford, Jong Wook Kim, Chris Hallacy, Aditya Ramesh, Gabriel Goh, Sandhini Agarwal, Girish Sastry, Amanda Askell, Pamela Mishkin, Jack Clark, et al. Learning transferable visual models from natural language supervision. In *ICML*, 2021. 1, 2, 3, 5
- [39] Ryan Razani, Ran Cheng, Enxu Li, Ehsan Taghavi, Yuan Ren, and Liu Bingbing. Gp-s3net: Graph-based panoptic sparse semantic segmentation network. In *ICCV*, 2021. 1
- [40] Kshitij Sirohi, Rohit Mohan, Daniel Büscher, Wolfram Burgard, and Abhinav Valada. Efficientlps: Efficient lidar panoptic segmentation. *IEEE Transactions on Robotics*, 38(3):1894–1914, 2021. 1
- [41] Haotian Tang, Zhijian Liu, Shengyu Zhao, Yujun Lin, Ji Lin, Hanrui Wang, and Song Han. Searching efficient 3d architectures with sparse point-voxel convolution. In *ECCV*, 2020. 2
- [42] Ashish Vaswani, Noam Shazeer, Niki Parmar, Jakob Uszkoreit, Llion Jones, Aidan N Gomez, Łukasz Kaiser, and Illia Polosukhin. Attention is all you need. In *NeurIPS*, 2017. 1, 5
- [43] Wenxuan Wu, Li Fuxin, and Qi Shan. Pointconvformer: Revenge of the point-based convolution. In *CVPR*, 2023. 2
- [44] Zeqi Xiao, Wenwei Zhang, Tai Wang, Chen Change Loy, Dahua Lin, and Jiangmiao Pang. Position-guided point cloud panoptic segmentation transformer. *arXiv preprint*, 2023. 1, 2, 3, 4, 5, 6, 7, 8, 11, 13
- [45] Jianyun Xu, Ruixiang Zhang, Jian Dou, Yushi Zhu, Jie Sun, and Shiliang Pu. Rpvnet: A deep and efficient range-point-voxel fusion network for lidar point cloud segmentation. In *ICCV*, 2021. 2
- [46] Jiarui Xu, Shalini De Mello, Sifei Liu, Wonmin Byeon, Thomas Breuel, Jan Kautz, and Xiaolong Wang. Groupvit: Semantic segmentation emerges from text supervision. In *CVPR*, 2022. 2
- [47] Jiarui Xu, Sifei Liu, Arash Vahdat, Wonmin Byeon, Xiaolong Wang, and Shalini De Mello. Open-vocabulary panoptic segmentation with text-to-image diffusion models. In *CVPR*, 2023. 1, 2, 6, 11
- [48] Mengde Xu, Zheng Zhang, Fangyun Wei, Yutong Lin, Yue Cao, Han Hu, and Xiang Bai. A simple baseline for open-vocabulary semantic segmentation with pre-trained vision-language model. In *ECCV*, 2022. 2
- [49] Shuangjie Xu, Rui Wan, Maosheng Ye, Xiaoyi Zou, and Tongyi Cao. Sparse cross-scale attention network for efficient lidar panoptic segmentation. In *AAAI*, 2022. 1
- [50] Jihan Yang, Runyu Ding, Zhe Wang, and Xiaojuan Qi. Regionplc: Regional point-language contrastive learning for open-world 3d scene understanding. *arXiv preprint arXiv:2304.00962*, 2023. 1, 2, 6, 7, 13
- [51] Qihang Yu, Ju He, Xueqing Deng, Xiaohui Shen, and Liang-Chieh Chen. Convolutions die hard: Open-vocabulary segmentation with single frozen convolutional clip. In *NeurIPS*, 2023. 1, 2, 3, 4, 5, 6, 11, 12
- [52] Junbo Zhang, Runpei Dong, and Kaisheng Ma. Clip-fo3d: Learning free open-world 3d scene representations from 2d dense clip. *arXiv preprint arXiv:2303.04748*, 2023. 1, 2
- [53] Chong Zhou, Chen Change Loy, and Bo Dai. Extract free dense labels from clip. In *ECCV*, 2022. 2
- [54] Zixiang Zhou, Yang Zhang, and Hassan Foroosh. Panoptic-polarnet: Proposal-free lidar point cloud panoptic segmentation. In *CVPR*, 2021. 1, 2
- [55] Ziqin Zhou, Yinjie Lei, Bowen Zhang, Lingqiao Liu, and Yifan Liu. Zegclip: Towards adapting clip for zero-shot semantic segmentation. In *CVPR*, 2023. 2
- [56] Xueyan Zou, Zi-Yi Dou, Jianwei Yang, Zhe Gan, Linjie Li, Chunyuan Li, Xiyang Dai, Harkirat Behl, Jianfeng Wang, Lu Yuan, et al. Generalized decoding for pixel, image, and language. In *CVPR*, 2023. 2

## A. PFC Baseline

As there is no existing work for the 3D open vocabulary panoptic segmentation task, a natural idea would be to extend the 2D state-of-the-art open vocabulary segmentation to 3D. We start by adapting the essential components from FC-CLIP [51], a 2D open-vocabulary segmentation model that achieves state-of-the-art performances across different datasets, to P3Former [44], a state-of-the-art 3D closed-set panoptic segmentation model. Since the models of FC-CLIP and P3Former are very different, we conduct some necessary changes to the architecture of P3Former. We name this baseline PCFormer+FC-CLIP (PFC). The overall architecture of the PFC is shown in Fig. 5.

**Vision CLIP feature extraction.** FC-CLIP[51] demonstrates that frozen CLIP features can produce promising classification performance on both base and novel classes. In the same spirit of this, we construct a Vision CLIP feature extractor as follows: a pre-trained V-L segmentation model [13] is applied to extract pixel-wise CLIP features from each camera image. Within each voxel, every LiDAR point is projected into its corresponding camera image based on the intrinsic and extrinsic calibration parameters, in order to index into the corresponding vision CLIP features. The vision CLIP features of all the points belonging to each voxel are then averaged to represent that voxel. The voxel CLIP features will be referred as  $F_{vclip} \in \mathbb{R}^{V \times D_{emb}}$ , where  $V$  is the number of voxels after voxelization and  $D_{emb}$  is the dimension of the CLIP features. Note that the Vision CLIP encoder is frozen and it is identical to the one in our proposed method.

**Segmentation head.** We use learnable queries  $q$  to represent each instance or thing. Queries matched with groundtruth objects are supervised with both classification loss and mask loss. FC-CLIP [51] shows that the mask generation is class-agnostic, and therefore we follow FC-CLIP and only modify the classification head to add a class embedding. Specifically, the class embedding  $f_{cls}$  prediction is defined as:

$$v_q = f_{cls}(q) \in \mathbb{R}^{D_{emb}}, \quad (9)$$

where  $v_q$  is in the CLIP embedding space. The predicted class logits are then computed from the cosine similarity between the predicted class embedding and the text embedding of every category name from the evaluation set using a frozen CLIP model. The classification logits are defined as:

$$s_{w_q} = \frac{1}{T} [\cos(v_q, t_1), \cos(v_q, t_2), \dots, \cos(v_q, t_C)] \quad (10)$$

where  $t_i \in \mathbb{R}^{D_{emb}}$ ,  $i \in \{1, 2, \dots, C\}$  is the text embedding,  $C$  is the number of categories ( $C_B$  in training and  $C_B + C_N$  in testing), and  $T$  is a learnable temperature term that controls the concentration of the distribu-

tion. Following FC-CLIP, we name this trainable classifier the **in-vocabulary** classifier. The loss function, then, is  $L = w_\alpha * L_{cls} + w_\beta * L_{mask}$ , where  $L_{cls}$  and  $L_{mask}$  are the softmax cross-entropy classification loss and mask loss, respectively.  $w_\alpha$  and  $w_\beta$  are weights for classification loss and mask loss, respectively. Note that, for classification, we apply a softmax cross-entropy loss instead of focal loss because of the following ensembling process.

**Geometric ensemble.** Previous open-vocabulary works [13, 14, 23, 47, 51] show that a trainable in-vocabulary classifier fails to make good predictions for novel classes. During testing, we follow [47, 51], and construct an **out-of-vocabulary** classifier that utilizes voxel Vision CLIP features to get an embedding for each query  $q$  by mask pooling the Vision CLIP features:

$$w_q = \frac{1}{|M_q|} \sum_p \mathbb{1}(p \in M_q) F_{vclip}(p) \quad (11)$$

, where  $M_q$  is the set of points,  $p$ , belonging to the mask for query,  $q$ . The out-of-vocabulary classification logits  $s_{w_q}$  can be computed as

$$s_{w_q} = \frac{1}{T} [\cos(v_q, t_1), \cos(v_q, t_2), \dots, \cos(v_q, t_C)] \quad (12)$$

where the temperature term  $T$  is the same as the one in Eq. (10). Note that the out-of-vocabulary classifier is frozen and is only applied during testing. The final classification score is computed as the geometric ensemble of the in-vocabulary classifier and out-of-vocabulary classifier for every class,  $i$ :

$$s_{g_q}(i) = \begin{cases} p_{v_q}(i)^{1-\alpha} p_{w_q}(i)^\alpha & \text{if } i \in C_B \\ p_{v_q}(i)^{1-\beta} p_{w_q}(i)^\beta & \text{if } i \in C_N \end{cases} \quad (13)$$

where  $p_{v_q} = \text{softmax}(s_{v_q})$ ,  $p_{w_q} = \text{softmax}(s_{w_q})$  are the derived probabilities and  $\alpha, \beta \in [0, 1]$  are hyperparameters to control the contributions of in-vocabulary classifier and out-of-vocabulary classifier. In practice, we try multiple pairs of  $\alpha, \beta$  and report the result of the best pair. We have found that  $\alpha = 0$  and  $\beta = 1$  generates the best results for the PFC baseline in all different base/novel splits, which indicates that the baseline solely relies on out-of-vocabulary classifier to make predictions for novel classes.

## B. Query Assignment

For both the baseline and our method, a single query is used to represent an individual object. This requires specific query assignment strategies to match predictions with groundtruth base objects during training. FC-CLIP uses one set of learnable queries to make predictions for base and novel classes. Therefore, the same set of queries are matched with base *thing* and *stuff* objects. The unmatched

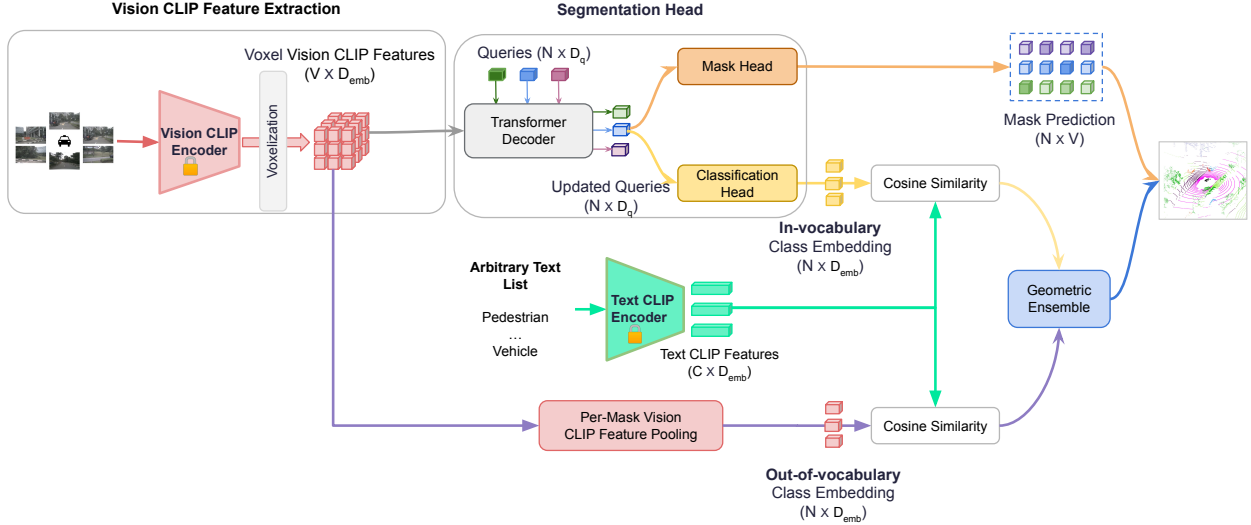


Figure 5. The overview of PFC baseline. The PFC baseline takes frozen voxel vision CLIP features as inputs. We modified the segmentation head of a close-set model so that it can predict in-vocabulary classes embedding. The classification score is predicted by computing the cosine similarity between the predicted embedding and the text CLIP embedding. During testing, we further apply per-mask vision feature pooling to obtain out-of-vocabulary class embedding. The final per-mask classification logits are the geometric ensemble of in-vocabulary and out-of-vocabulary classification results.

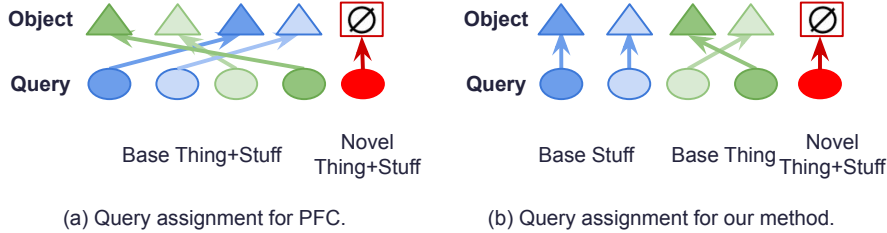


Figure 6. Visualization for the two strategies for query assignment.

queries are potentially in charge of making predictions for novel *thing* and *stuff* objects, as shown in Fig. 6 (a). In contrast, our method uses two sets of queries. The first query set is used to represent base *things* classes after bipartite matching, while the second, fixed, query set is for base *stuff* classes, as shown in Fig. 6 (b). The separation of base *things* queries and base *stuff* queries makes our model converge faster and improves overall performance.

### C. More Experimental Results

**Queries in object-level distillation loss.** In our loss function design for the object-level distillation loss,  $L_O$ , we only enforce constraints on queries matched with base classes. One natural question would be: can we apply the constraint on all queries to improve predictions? We conduct an ablation study for this, with results shown in Tab. 6. When we apply the object-level distillation loss to all queries, the overall performance is slightly worse, especially for the novel *stuff* classes.

**More splits.** In order to show that our proposed method

generalizes well in different scenarios, we conduct experiments on two more random B12/N4 splits. As shown in Tab. 7 and Tab. 8, our method surpasses the PFC baseline in almost all metrics across all the splits, demonstrating the capability of our proposed method.

**Performance on novel stuff classes.** The performance of PFC baseline is almost 0 on novel *stuff* classes. To verify whether it is due to poor mask predictions for the novel stuff classes, we conduct an oracle experiment by max-pooling vision CLIP features with ground truth masks and then use its similarity with CLIP text features to determine its category, and the results are shown in Tab. 9. We achieve 53 RQ using ground truth mask, which demonstrate that the bad performance of PFC baseline is indeed due to poor mask quality. Also, the low RQ number shows that the prediction task on novel stuff class is very challenging.

### D. Discussion

**Class-agnostic mask generator.** As shown in FC-CLIP [51], the mask head is class-agnostic if we do not

Queries in $L_O$	$PQ$	$PQ_N^{Th}$	$PQ_N^{St}$	$RQ$	$RQ_N^{Th}$	$RQ_N^{St}$	$SQ$	$SQ_N^{Th}$	$SQ_N^{St}$	mIoU
Matched Only	<b>62.0</b>	49.6	<b>35.2</b>	<b>70.9</b>	55.6	<b>46.0</b>	<b>87.0</b>	89.1	<b>76.7</b>	<b>60.1</b>
All	61.0	<b>49.9</b>	25.4	70.0	<b>56.3</b>	34.4	86.3	74.3	88.7	60.5

Table 6. **Impact of queries in  $L_O$ .** We conduct an ablation study comparing applying  $L_O$  to matched queries vs all queries. The overall performance is better when we only apply  $L_O$  on matched queries.

Model	Type	Supervision	$PQ$	$PQ_N^{Th}$	$PQ_N^{St}$	$RQ$	$RQ_N^{Th}$	$RQ_N^{St}$	$SQ$	$SQ_N^{Th}$	$SQ_N^{St}$	mIoU
P3Former[44]	closed-set	full	75.8	76.4	86.9	83.8	84.8	98.3	90.1	89.8	88.4	78.2
PFC	open-voc	partial	49.9	22.5	14.0	59.6	<b>26.9</b>	21.9	85.6	82.9	61.0	53.8
Ours	open-voc	partial	<b>55.4</b>	<b>23.2</b>	<b>24.7</b>	<b>62.9</b>	26.0	<b>29.8</b>	<b>85.6</b>	<b>87.6</b>	<b>69.3</b>	<b>55.0</b>

Table 7. **Performance of panoptic segmentation on nuScenes with a different split.** We compare the performance with a different split with 4 novel classes (B12/N4). The novel *things* classes are construction vehicle and traffic cone. The novel *stuff* classes are other-flat and man-made. Our method consistently outperforms the PFC baseline across almost all the metrics by a large margin.

Model	Type	Supervision	$PQ$	$PQ_N^{Th}$	$PQ_N^{St}$	$RQ$	$RQ_N^{Th}$	$RQ_N^{St}$	$SQ$	$SQ_N^{Th}$	$SQ_N^{St}$	mIoU
P3Former[44]	closed-set	full	75.8	71.1	96.2	83.8	78.8	99.9	90.1	90.1	96.3	78.2
PFC	open-voc	partial	43.1	16.4	2.1	51.6	20.0	3.0	79.8	83.8	<b>69.7</b>	43.5
Ours	open-voc	partial	<b>53.1</b>	<b>31.0</b>	<b>35.1</b>	<b>63.0</b>	<b>35.2</b>	<b>53.8</b>	<b>82.3</b>	<b>87.7</b>	65.3	<b>50.5</b>

Table 8. **Performance of panoptic segmentation on nuScenes with a different split.** We compare the performance with a different split with 4 novel classes (B12/N4). The novel *things* classes are barrier, bus and truck. The novel *stuff* class is drivable surface. Our method consistently outperforms the PFC baseline across almost all the metrics by a large margin.

	mIoU	PQ	RQ	SQ
PFC	4.38	0.5	0.83	60.44
Ours	45.14	35.25	45.97	76.69
Oracle (GT Masks)	51.39	52.61	53.00	99.26

Table 9. **Performance on novel *stuff* classes.** We compare the performance of PFC, our method and the oracle setting that based on the GT masks on novel *stuff* classes. The splits are the same as in Tab. 1.

apply any penalty to unmatched queries. We follow the same strategy in our paper. The metrics  $SQ_N^{Th}$  and  $SQ_N^{St}$  in all experiments indicate that the mask predictions for both *things* and *stuff* are reasonable.

**Comparison with RegionPLC.** RegionPLC [50] proposes to take advantage of regional visual prompts to create dense captions. After point-discriminative contrastive learning, the model can be used for semantic segmentation or instance segmentation. There are two main differences between RegionPLC and our method: 1. RegionPLC addresses the problem of semantic segmentation or instance segmentation individually, while our model addresses semantic segmentation and instance segmentation in the same model. 2. RegionPLC focuses on getting point-level discriminative features, while our model takes the pretrained CLIP features as input and aims to build model architecture and design loss functions. In our method, we do not compare with RegionPLC because the experiment settings

are different and there is no public code to reproduce the contrastive learning process. However, we do think there is great potential in combining RegionPLC and our method. One idea would be to replace the vision CLIP features in our model with the features derived from RegionPLC.

## E. Visualization

We present the visualization of PFC baseline, our method and groundtruth in Fig. 7 and Fig. 8. Note that we only visualize the points that are visible in frontal camera views in Fig. 8.

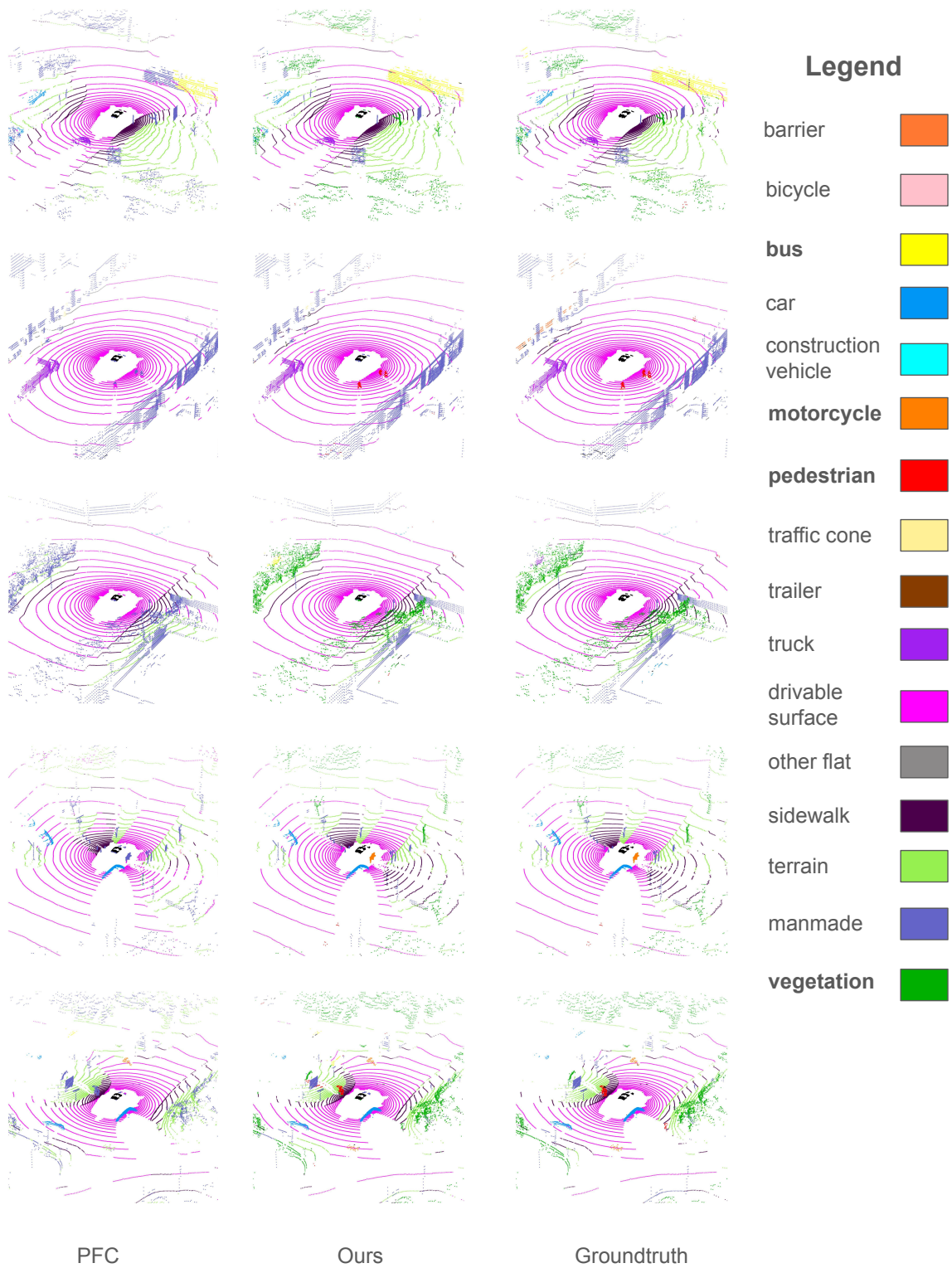


Figure 7. Qualitative Results in nuScenes Dataset. We present the comparison among PFC, our method and the groundtruth. The novel objects are marked in **bold** in the legend.

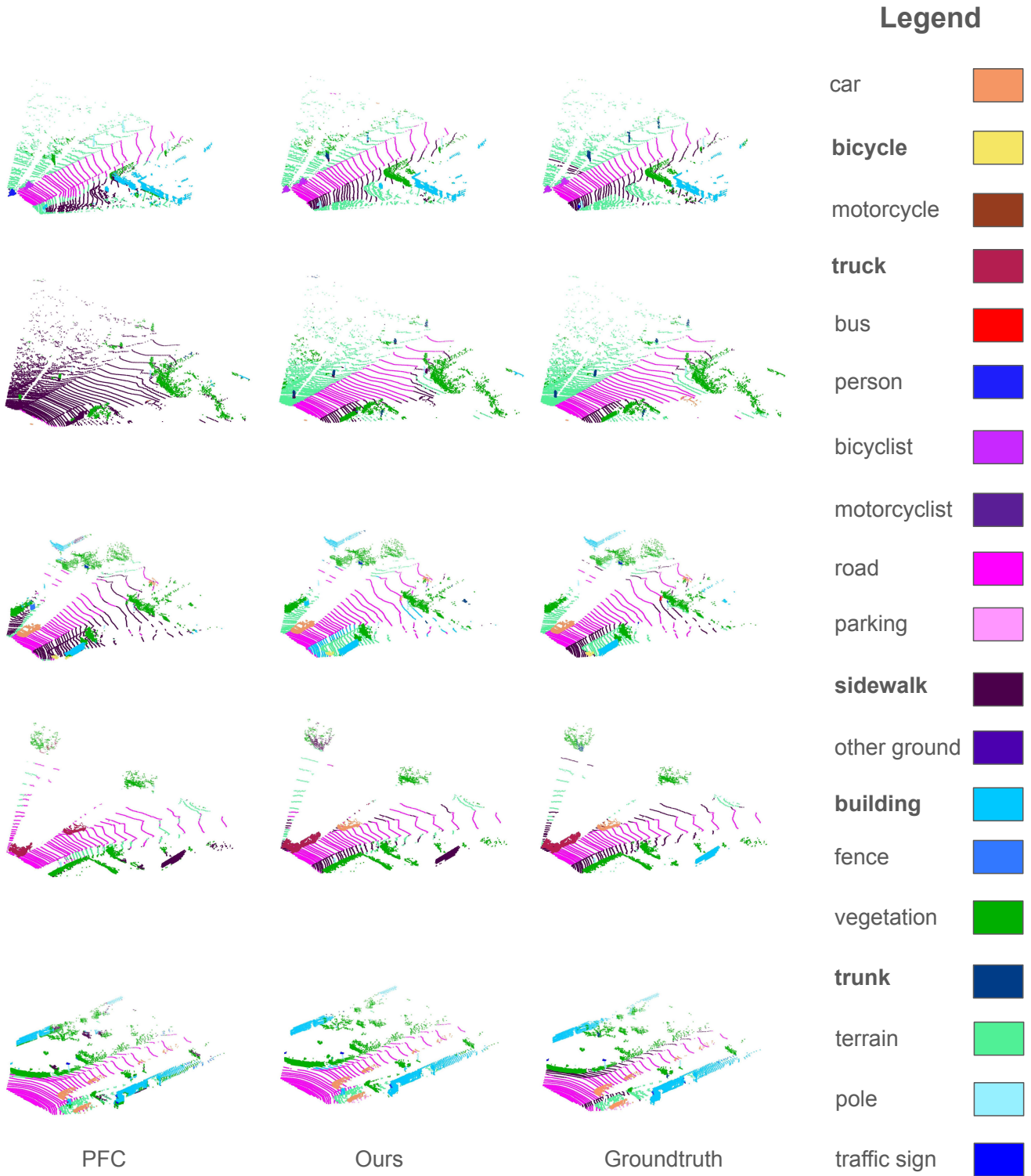


Figure 8. Qualitative Results in SemanticKITTI Dataset. We present the comparison among PFC, our method and the groundtruth. The novel objects are marked in **bold** in the legend.